HHS Public Access

Author manuscript

*Nat Med*. Author manuscript; available in PMC 2018 December 03.

Published in final edited form as:

*Nat Med*. 2017 June ; 23(6): 763–767. doi:10.1038/nm.4322.

# A live-attenuated Zika virus vaccine candidate induces sterilizing immunity in mouse models

**Chao Shan**[1], **Antonio E. Muruato**[2,3], **Bruno T.D. Nunes**[1,4], **Huanle Luo**[5], **Xuping Xie**[1], **Daniele B.A. Medeiros**[1,4], **Maki Wakamiya**[1], **Robert B. Tesh**[2,6], **Alan D. Barrett**[2,6,7], **Tian Wang**[5,6,7], **Scott C. Weaver**[2,3,5,7,9], **Pedro F.C. Vasconcelos**[4,10], **Shannan L. Rossi**[2,6,*], and **Pei-Yong Shi**[1,7,8,9,*]

[1]Department of Biochemistry & Molecular Biology, Galveston, Texas, USA

[2]Institute for Human Infections & Immunity, Galveston, Texas, USA

[3]Institute for Translational Science, Galveston, Texas, USA

[4]Seção de Arbovirologia e Febres Hemorrágicas, Instituto Evandro Chagas, Ministério da Saúde, Ananindeua, Pará, Brazil

[5]Department of Microbiology & Immunology, University of Texas Medical Branch, Galveston, Texas, USA

[6]Department of Pathology and Center for Biodefense & Emerging Infectious Diseases, University of Texas Medical Branch, Galveston, Texas, USA

[7]Sealy Center for Vaccine Development, University of Texas Medical Branch, Galveston, Texas, USA

[8]Department of Phamarcology & Toxicology, University of Texas Medical Branch, Galveston, Texas, USA

[9]Sealy Center for Structural Biology & Molecular Biophysics, University of Texas Medical Branch, Galveston, Texas, USA

[10]Department of Pathology, Pará State University, Belém, Brazil

## Abstract

Zika virus (ZIKV) infection of pregnant patients could cause a wide range of congenital abnormalities (including microcephaly) now collectively known as congenital ZIKV syndrome[1]. A vaccine to prevent or significantly attenuate viremia in pregnant women and travelers to epidemic/endemic regions is needed to avert congenital ZIKV syndrome, and could also be useful to suppress epidemic transmission. Here we report a live-attenuated vaccine candidate that contains a 10-nucleotide deletion in the 3' untranslated region of ZIKV genome (10-del ZIKV). The 10-del

*Correspondence: PYS (peshi@utmb.edu) or SLR (slrossi@utmb.edu).

AUTHOR CONTRIBUTIONS

C.S., A.E.M., B.T.D.N., H.L., X.X., and D.B.A.M. performed experiments and data analysis. M.W., R.B.T., A.D.B., S.C.W., P.F.C.V., T.W., S.L.R., and P.Y.S. designed the experiments and interpreted the results. C.S., A.E.M., T.W., S.C.W., P.F.C.V., S.R., and P.Y.S. wrote the manuscript.

CONFLICT OF INTEREST STATEMENT

The authors have no conflict of interest in this study.

ZIKV is highly attenuated, immunogenic, and protective in the A129 mouse model. Critically, a single dose of 10-del ZIKV induced sterilizing immunity with a high level of neutralizing antibodies and completely prevented viremia after challenge. The immunized mice also developed a robust T cell response. Intracranial inoculation of one-day-old CD1 mice with $1\times10^4$ IFU of 10-del ZIKV caused no detectable disease, whereas infections with 10 IFU of wild-type ZIKV were lethal. Mechanistically, the 10-del ZIKV attenuated its virulence through decreased viral RNA synthesis and increased sensitivity to type-I interferon inhibition. The attenuated 10-del ZIKV was incompetent in infecting mosquitoes after oral feeding of spiked blood meals, representing an additional safety feature for use in non-endemic regions. Collectively, the safety and efficacy results warrant further development of this promising live-attenuated ZIKV vaccine candidate.

**Keywords**

Zika virus; vaccine; flavivirus; emerging virus

The mosquito-borne ZIKV has recently caused a global threat to public health. Prevention of congenital ZIKV syndrome is the most pressing task to reduce the burden of epidemics on family and society[2]. An effective vaccine is urgently needed for both the general population in epidemic/endemic countries to suppress transmission and for travelers to those regions. Both inactivated and live-attenuated vaccines have been developed for flaviviruses, including yellow fever (YFV), Japanese encephalitis (JEV), tick-borne encephalitis (TBEV), and dengue (DENV) viruses[3]. Rapid and promising progress has been made toward ZIKV vaccine development[4,5]. Inactivated ZIKV and subunit vaccines (expressing viral prM/E proteins) have shown efficacy in mice and nonhuman primates[6–8], but to date there have been no reports on candidate live attenuated vaccines (LAVs). We chose to pursue a LAV to capitalize on its advantages of single-dose immunization, rapid and robust immune response, and long-lived protection. We attenuated wild-type (WT) ZIKV through deletion of a portion of the 3’ untranslated region (3’UTR) of the viral genome. A similar approach has been successfully used to develop a DENV vaccine currently in a phase III clinical trial[9].

Using an infectious cDNA clone of the ZIKV Cambodian strain FSS13025[10] (a non-epidemic strain, but phylogenetically closely related to strains now circulating in the Americas), we prepared a panel of recombinant viruses containing distinct 3’UTR deletions (Fig. 1a). Mutants 10-del, 20-del, 30-del-a, and 30-del-b contained overlapping 10-to-30-nucleotide deletions, which were expected to change the local secondary structure of the viral 3’UTR (Extended Data Fig. 1). Upon transfection into Vero cells, all mutant genomic RNAs generated viral E protein-expression cells (Extended Data Fig. 2) and infectious viruses (defined as P0 viruses). Compared with the WT, all mutants exhibited smaller infectious foci (Fig. 1b), slower replication kinetics, and lower peak titers (Fig. 1c). To examine the mutational effects on viral replication, we engineered the deletions into a luciferase ZIKV replicon[11]. The replicon results showed that the 3’UTR deletions did not affect viral RNA translation (indicated by the luciferase signals at 2–6 h post-transfection), but decreased RNA synthesis (indicated by the luciferase activities at 24–48 h post-transfection; Fig. 1d); a similar observation was previously reported for West Nile virus, a closely related flavivirus[12]. Since the 3’UTR of flaviviruses may also modulate host innate

immune response[13,14], we compared the susceptibility of the WT and mutant viruses to interferon inhibition. All four mutant viruses were much more sensitive to interferon-β inhibition than the WT virus, among which mutant 10-del exhibited the greatest inhibition (Fig. 1e). Collectively, these results indicate that 3'UTR deletions attenuate ZIKV replication through diminished viral RNA synthesis and increased vulnerability to type-I interferon inhibition.

To test the stability of the mutant viruses, we passaged them five times on Vero cells (an approved cell line for vaccine production[15]; 5 days per passage). The P5 viruses developed larger infectious foci (Extended data Fig. 3a) and faster replication kinetics than the corresponding P0 viruses on Vero cells (Compare Extended data Fig. 3b with Fig. 1c). Complete genome sequencing of P0 and P5 viruses showed that all mutants retained the original deletions, but the P5 viruses had accumulated additional mutations in the E and/or NS1 genes, which presumably were Vero cell-adaptive mutation(s) and/or compensatory mutation(s) to 3'UTR deletions (Extended data Fig. 3c). Further passaging of the mutant viruses on Vero cells to P20 did not change the engineered 3'UTR deletions (data not shown). The results indicated that the engineered deletions are stable when propagated on Vero cells.

We evaluated the immunogenicity and efficacy of the P0 mutant viruses in an A129 (interferon α/β receptor-deficient) mouse model[16] (Fig. 2a). After subcutaneous (S.C.) inoculation with $1\times10^4$ IFU of virus, mice infected with the WT virus had significantly more weight loss than those infected with mutant viruses; whereas the differences in mean weight loss among the four mutant virus-infected groups were not statistically significant (Fig. 2b). About 50% of the mice succumbed to the WT virus infection, whereas no mortality was observed in the mutant virus-infected mice (Fig. 2c). The WT virus produced significantly higher peak viremia than the mutant viruses, among which the 10-del virus had the lowest viremic profile (Fig. 2d). The viremia for 10-del mutant dropped to 700 IFU, 350 IFU, and undetectable on days 5, 6, and 7 post-infection, respectively (data not shown). Sequencing analysis confirmed that the engineered deletions were retained without other mutations in the mutant viruses recovered from the mouse sera (data not shown). On day 28 post-infection, mouse sera were taken and quantified for pre-challenge neutralization titers using an mCherry ZIKV (Extended Data Fig. 4). Comparable pre-challenge neutralization titers of $(1.8\pm1.1)\times10^3$ to $(8.6\pm1.5)\times10^3$ were observed among the WT and mutant virus-infected mice (Fig. 2e). After challenge with $1\times10^5$ IFU of WT ZIKV (Cambodian strain FSS13025) on day 28 post-immunization, the immunized mice had no detectable peripheral viremia, whereas the mock-immunized group produced a mean viremia of $(8.5\pm1.5)\times10^6$ IFU/ml on day 2 post-challenge (Fig. 2f). On day 28 post-challenge, we measured the neutralization titers of the mouse sera again; remarkably, the post-challenge neutralization titers were equivalent to the pre-challenge neutralization titers (compare Fig. 2e&g), suggesting that a sterilizing antibody response had been achieved by a single vaccination. Altogether, the results demonstrate that the mutant viruses are highly attenuated, immunogenic, and protective in A129 mice.

Since the 10-del virus produced the lowest viremia in mice (Fig. 2d), yet induced a neutralizing antibody response comparable to those of the WT and other mutants (Fig. 2e-g),

we prioritized this mutant for further characterization. At a dose of 100 IFU, 10-del virus-infected mice showed a delayed peak viremia that was >100-fold lower than that of the WT virus (Extended Data Fig. 5a). Equivalent levels of pre-challenge neutralization titers were induced by the WT and 10-del viruses (Extended Data Fig. 5b), leading to complete protection from viremia after challenge with $1\times10^6$ IFU of Puerto Rico ZIKV strain PRVABC59 (Extended Data Fig. 5c). Furthermore, even when immunized at a dose of only 10 IFU, 10-del virus-infected mice generated a neutralization titer of $(9.7\pm6.8)\times10^3$ and were fully protected from viremia after challenge (Extended Data Fig. 2). It is noteworthy that mice immunized with different doses of 10-del mutant (10, $10^2$, and $10^4$ IFU) induced similar neutralization antibody titers and completely prevented viremia upon challenge (compare Fig. 2 and Extended Data Figs. 5&6). Collectively, these results demonstrate that the 10-del virus is a potent vaccine candidate.

Since P5 virus accumulated Vero cell-adaptive mutations (Extended data Fig. 4c), we compared the virulence and immunogenicity between the P0 and P5 10-del viruses in the A129 mice. After immunization with 100 IFU virus via the S.C. route, the P0 and P5 viruses generated comparable viremia and induced equivalent neutralization titers (Extended Data Fig. 7a&b). After challenging with $1\times10^6$ IFU of Puerto Rico strain PRVABC59 ZIKV via the I.P. route, no viremia was detected in the P0 or P5 virus-vaccinated mice; in contrast, robust viremia were detected in the sham group (Extended Data Fig. 7c). These results indicate that the Vero cell-adaptive mutations recovered from the P5 virus do not significantly affect the virulence and immunogenicity of the 10-del virus.

Next, we analyzed the T cell responses in A129 mice immunized with $1\times10^4$ IFU of WT and 10-del viruses. On 28 day post-immunization, ZIKV-specific T cells were re-stimulated with live WT virus *in vitro*, and analyzed using an intracellular cytokine staining (ICS) assay and a Bio-Plex immunoassay. The results showed that both WT and mutant virus-immune $CD4^+$ and $CD8^+$ T cells had higher IFN-γ responses than the mock-immunized group (Fig. 3a&b). Furthermore, these immune T cells induced more IFN-γ (Fig. 3c) and IL2 (Fig. 3d) than the mock group; particularly, the 10-del mutant-immune T cells produced 4-fold higher IFN-γ than the WT virus-immune group. These results indicate that 10-del vaccine candidate induces a robust T cell response.

Three sets of experiments were performed to analyze the safety of the 10-del vaccine candidate. First, we measured the viral loads in different organs after S.C. inoculation of A129 mice with $1\times10^4$ IFU of WT or 10-del viruses (Fig. 4a). On day 6 post-infection, the WT-infected mice had high viral loads in all organs tested, whereas the 10-del-infected mice had no virus in muscle or brain, and lower viral loads in heart, lung, liver, spleen, kidney, testes, and eye. On day 10 post-infection, WT virus-infected mice retained viral loads in kidney, brain, testis, and eye, among which testes had the highest mean titer; in contrast, no virus could be detected ($\leq10^2$ IFU/ml) in any organs from the 10-del-infected mice, suggesting an organ-selective attenuation, possibly through unidentified cell-type-specific antiviral responses. Since ZIKV infection was reported to damage the testis in mice[17,18], we examined the effect of immunization on the function of testis in the A129 mice. On day 16 post-immunization, similar weight and size of testis were recovered from the mock-, WT virus-, and 10-del mutant-infected mice (data not shown). However, motile and total sperm

counts were reduced in the WT virus-infected mice, whereas the 10-del virus-infected mice did not significantly compromise the sperm counts when compared with the mock group (Fig. 4b). Second, we examined the neurovirulence of 10-del virus through intracranial (I.C.) injection of one-day-old CD1 mice (Fig. 4c). The newborn mice succumbed to WT virus infection in a dose-responsive manner; even a dose of 10 IFU resulted in 25% mortality. Remarkably, mice infected with 10-del virus did not show any apparent disease or death, even at a dose of $1\times10^4$ IFU. Finally, we determined if 10-del virus could infect *Aedes aegypti* mosquitoes, the main transmission vector of ZIKV in the Americas[19,20]. After exposure to artificial blood-meals containing $1\times10^6$ IFU/ml of WT or 10-del virus, and incubation for 7 days, 56% of the engorged mosquitoes were infected by the WT virus, whereas no mosquitoes were infected by the 10-del mutant (Fig. 4d). Furthermore, intrathorax injection of 10-del virus to mosquitoes did not yield any infectious virus on day 7 after injection (data not shown). Collectively, our results demonstrated that the 10-del virus significantly reduced or eliminated viral loads in mouse organs, decreased neurovirulence by >1,000-fold, and attenuated its ability to infect the principal urban mosquito vector, all suggestive of an excellent safety profile.

A successful vaccine requires a fine balance between immunogenicity and safety. Live-attenuated vaccines generally offer fast and durable immunity, but sometimes with the trade-off of reduced safety; whereas inactivated and subunit vaccines provide enhanced safety at the cost of reduced immunogenicity, and often require multiple doses and periodic boosters. Our data indicate that the 3'UTR 10-del ZIKV is a promising live-attenuated vaccine candidate with a good balance between immunogenicity and safety. A single immunization elicited robust antibody and T cell responses, and significantly, unlike the subunit and inactivated ZKV vaccines published to date, likely induces sterilizing immunity and providing complete protection against parental and epidemic strains of ZIKV. Vaccine-induced sterilizing immunity is likely critical for a successful ZIKV vaccine to prevent viremia and congenital abnormalities. The safety profile of this vaccine candidate is highlighted by the low viremia, little and transient viral loads in organs, and limited weight loss in the severe A129 mouse model, as well as a complete lack of morbidity and mortality in one-day-old mice after receiving an I.C. injection. The latter safety result is impressive because I.C. inoculation with YFV 17D and JEV SA14–14-2 (two licensed live-attenuated flavivirus vaccines) results in lethal disease in one-day-old newborn mice[21,22]. Although potential homologous recombination between the WT and vaccine ZIKVs might pose a safety liability for the 10-del vaccine candidate, it should be noted that recombination events are rare and could not be detected in cell culture[23–27]. Compared with the chimeric, live-attenuated ZIKV vaccine (e.g., YFV 17D expressing ZIKV prM-E or DENV expressing ZIKV prM-E[28]), our 3'UTR mutant vaccine has the advantage of retaining all ZIKV structural and nonstructural genes that may contribute to antiviral protection, as indicated from dengue vaccine studies[29,30]. Mechanistically, the 3'UTR mutant viruses appeared to be attenuated through decreased viral RNA replication and increased sensitivity to type-I interferon inhibition. The latter mechanism is in agreement with a recent report that genetic diversity at the 3'UTR of DENV contributes to epidemic potential[14]. Future studies are needed to understand why larger 3'UTR deletion mutants (20-del and 30-del) were less attenuated than the 10-del mutant and whether these larger deletion mutants were competent

in infecting mosquitoes. Taken together, our results indicate that the 3'UTR mutant ZIKV is an attractive vaccine candidate that should be advanced to non-human primates for further development.

## METHODS

### Cells, viruses, and antibodies.

Vero cells were purchased from the American Type Culture Collection (ATCC, Bethesda, MD), and maintained in a high glucose Dulbecco modified Eagle medium (DMEM) (Invitrogen, Carlsbad, CA) supplemented with 10% fetal bovine serum (FBS) (HyClone Laboratories, Logan, UT) and 1% penicillin/streptomycin (Invitrogen, Carlsbad, CA) at 37°C with 5% $CO_2$. The following antibodies were used in this study: a mouse monoclonal antibody (mAb) 4G2 cross-reactive with flavivirus E protein (ATCC), ZIKV-specific HMAF [hyper-immune ascitic fluid, World Reference Center of Emerging Viruses and Arboviruses (WRCEVA) at the University of Texas Medical Branch], Anti-Mouse IgG (H+L) Antibody Horseradish Peroxidase-labeled (KPL, Gaithersburg, MD), and goat anti-mouse IgG conjugated with Alexa Fluor 488 (Thermo Fisher Scientific). The ZIKV Cambodian strain FSS13025 (GenBank number KU955593.1) was generated from an infectious cDNA clone pFLZIKV as described previously[10]. The Puerto Rico strain PRVABC59 (GenBank number KU501215) was obtained from WRCEVA. All the cell lines are tested negative for mycoplasma.

### Plasmid construction.

Standard molecular biology procedures were performed for all plasmid constructions. Standard overlap PCR was performed to amplify the DNA fragment between unique restriction enzyme sites EcoRI and ClaI using corresponding primer pairs. The DNA fragment containing 3'UTR deletion mutations were individually introduced into the pFLZIKV and pZIKV Rep (replicon cDNA plasmid[11]) through EcoRI and ClaI. The construction of the cDNA clone for mCherry ZIKV will be reported elsewhere. All the constructs were verified by DNA sequencing. Primer sequences are available upon request. All restriction enzymes were purchased from New England BioLabs (Ipswitch, MA).

### RNA transcription and transfection.

Full-genome ZIKV, mCherry ZIKV, and replicon RNAs were *in vitro* transcribed using a T7 mMessage mMachine kit (Ambion, Austin, TX) from cDNA plasmids pre-linearized by ClaI. The RNA was precipitated with lithium chloride, washed with 70% ethanol, re-suspended in RNase-free water, quantitated by spectrophotometry, and stored at −80°C in aliquots. The RNA transcripts (10 μg) were electroporated into Vero cells following a protocol described previously[31].

### Indirect immunofluorescence assays (IFA).

Vero cells transfected with viral RNA were grown in an 8-well Lab-Tek chamber slide (Thermo Fisher Scientific, Waltham, MA). At indicated time points, the cells were fixed in 100% methanol at −20°C for 15 min. After 1 h incubation in a blocking buffer containing 1% FBS and 0.05% Tween-20 in PBS, the cells were treated with a mouse monoclonal

antibody 4G2 for 1 h and washed three times with PBS (5 min for each wash). The cells were then incubated with Alexa Fluor® 488 goat anti-mouse IgG for 1 h in blocking buffer, after which the cells were washed three times with PBS. The cells were mounted in a mounting medium with DAPI (4', 6-diamidino-2-phenylindole; Vector Laboratories, Inc.). Fluorescence images were observed under a fluorescence microscope equipped with a video documentation system (Olympus).

### Luciferase assay.

The luciferase assay was performed as previously reported[11]. Briefly, Vero cells transfected with WT or mutant ZIKV replicon RNAs (10 μg) were seeded in a 12-well plate. At various time points, the cells were washed once with phosphate-buffered saline (PBS) and lysed using cell lysis buffer (Promega, Madison, WI). The cells were scraped from plates and stored at −80°C. The luciferase signals were measured by Cytation 5 (Biotek) according to the manufacturer's instructions.

### Stability of 3'UTR mutants, RNA extraction, and RT-PCR.

To examine the stability of 3'UTR mutants, we passaged them on Vero cells for five rounds. Briefly, $1.5\times10^6$ Vero cells were seeded into T-25 flask. The virus derived from RNA transfection, defined as P0 was used to infect the Vero cells. At 5 d p.i., culture fluid (100 μl) was transferred to a new T-25 flask containing Vero cells in 5 ml of culture medium. After five rounds of such passaging (P5), viral RNAs were extracted from the P5 culture fluids using QIAamp Viral RNA Kit (Qiagen). Viral RNAs were amplified by RT-PCR using SuperScript III one-step RT-PCR kits (Invitrogen). The P5 viruses were subjected to complete genome-length sequencing. Three independent passages were performed for each mutant virus.

### Immunostaining focus assay and immunostaining.

Viral samples were ten-fold serially diluted six times in DMEM. For each dilution, 100 μl sample was added to a 24-well plate containing Vero cells at about 90% confluency. The infected cells were incubated for 1 h and swirled every 15 min to ensure complete coverage of the monolayer for even infection. After 1 h incubation, 0.5 ml of methyl cellulose overlay containing 2% FBS 1% penicillin/streptomycin was added to each well. The plate was incubated at 37°C for four days. Following the incubation, methyl cellulose overlay was removed and 0.5 ml methanol-acetone (1:1) solution was added into each well and incubated at room temperature for 15 min. Fixation solution was aspirated and plates were allowed to air dry, then washed three times with PBS and incubated in blocking buffer (PBS supplemented with 3% FBS), followed by 1 h incubation with ZIKV-specific HMAF. Plates were washed three times with PBS followed by an hour-long incubation with a secondary antibody conjugated to horseradish peroxidase (KPL, Gaithersburg, MD). Detection proceeded with the addition of aminoethylcarbazole substrate (ENZO Life sciences, Farmingdale, MA) prepared according to the vendor's instructions.

### Replication curves.

Subconfluent Vero cells in 12-well plates were infected with either P0 or P5 ZIKV at an multiplicity of infection (MOI) of 0.01 in triplicate wells. Virus stocks were diluted in DMEM containing 2% FBS and 1% penicillin/streptomycin. One hundred microliters of virus were added to each well of the 12-well plates. After 1 h attachment (5% $CO_2$ at 37°C), the inocula were removed, monolayers were washed three times with PBS, and 1 ml DMEM medium containing 2% FBS and 1% penicillin/streptomycin was added to each well. The plates were incubated for up to 5 days and medium was collected daily for immunostaining focus assay as described above.

### Vaccination and challenge of mice.

All animal testing was performed in accordance UTMB policy as approved by the UTMB IACUC. Three-week old A129 mice were immunized by the subcutaneous (S.C.) route with $1\times10^4$ IFU, $1\times10^2$ IFU, or 10 IFU WT or mutant viruses. Mock-infected mice were given PBS by the same route. Mice were weighed and monitored daily for progression of disease. Mice were anesthetized and bled via the retro orbital sinus (R.O.) every two days. On day 28 post-immunization, mice were anesthetized and bled to measure neutralization antibody titers using a mCherry ZIKV infection assay. The vaccinated mice were then challenged via the intraperitoneal (I.P.) route with either FSS13025 at $1\times10^5$ IFU or PRVABC59 at $1\times10^6$ IFU. On day 2 post-challenge, the mice were bled to measure viremia. Blood was clarified post collection by centrifugation at 3,380 × g for 5 min and immediately stored at −80°C for storage. Viral titers of sera and inoculum were determined by an immunostaining focus assay on Vero cells as described above.

### Neurovirulence on newborn CD1 mice.

Groups of 1-day-old outbred CD1 mice (n=7–10) were injected intracranially (I.C.) with WT or 10-del with serial tenfold dilutions from 10,000 IFU to 10 IFU. Mice were monitored daily for morbidity and mortality.

### Organ virus titers.

The heart, lung, liver, spleen, kidney, muscle, brain, testis, and eye were harvested on day 6 and 10 post-infection after $1\times10^4$ IFU of WT and del-10 virus vaccination via the S.C. route. Organ titrations were performed using a immunostaining focus assay as described above. In brief, 500 μl of DMEM with 2% FBS and penicillin/streptomycin along with a steel ball bearing were placed in a 2-ml Eppendorf tube. The organ (whole or part) was placed in the tube. Tubes were weighed, and organ weight was determined by subtracting the tube weight. Tissues were homogenized in a Qiagen TissueLyser II shaking at 26 p/second for 5 minutes. The homogenate was clarified by centrifugation for 5 min at 12,000 rpm and titrated on Vero monolayer using an immunostaining focus assay. The titer was then adjusted for volume and organ weight to report the organ loads as IFU/g[16].

### Testis and sperm count analyses.

A129 mice were infected with $1\times10^4$ IFU of WT or 10-del mutant virus. A mock-infected group with PBS was included as a negative control. On day 16 p.i., the mice were

euthanized and necropsied; epididymis and testes were harvested immediately as previously described[32]. Briefly, the epididymis was placed into 1 ml of pre-warmed M2 media at 37°C. To release the sperm, the epididymis was cut lengthwise six times and incubated for 10 min, agitating every 2 min at 37°C. Following the incubation, the media containing the sperm was immediately diluted 1:50 into pre-warmed M2 media and counted on a hemocytometer. Motile sperms were categorized into progressive and non-progressive. Progressively motile sperms are described as continuous displacement of the head by flagellar movement. Non-progressively motile sperms are described as little to no displacement of the head by flagellar movement. In the non-motile sperms, no flagellar movement was observed.

### Antibody neutralization assay.

Neutralizing activity of mouse sera was assessed using a newly established mCherry ZIKV. The sera were 2-fold serially diluted starting at 1:100 in DMEM with 2% FBS and 1% penicillin/streptomycin. Serial dilution of mice sera was incubated with mCherry ZIKV at 37°C for 2 h. Antibody-virus complexes were added to pre-seeded Vero cells in 96-well plates. After 48 h post-infection, cells were visualized by fluorescence microscopy using Cytation 5 Cell Imaging Multi-Mode Reader (Biotek) to quantify the mCherry fluorescence-positive cells. The percentage of fluorescence-positive cells in the non-treatment controls was set at 100%. The fluorescence-positive cells from serum-treated wells were normalized to those of non-treatment controls. A four-parameter sigmoidal (logistic) model in the software GraphPad Prism 7 was used to calculate the neutralization titers ($NT_{50}$).

### Experimental infection of mosquitoes with ZIKV.

*Aedes aegypti* mosquitoes derived from a Galveston, Texas colony were exposed for 45 min to blood-meals consisting of 1% (weight/volume) sucrose, 20% (vol/vol) FBS, 5 mM ATP, 33% (vol/vol) PBS-washed human blood cells (UTMB Blood Bank), and 33% (vol/vol) DMEM medium and combined with 1 ml virus offered in Hemotek 2-ml heated reservoirs (Discovery Workshops) covered with a mouse skin. Virus titers in the blood meals were $1\times10^6$ IFU/ml. Infectious blood meals were loaded on cartons containing *Ae. aegypti*. Fully engorged mosquitoes were incubated at 28°C, 80% relative humidity on a 12:12 h light:dark cycle with *ad lib* access to 10% sucrose solution for 7 days and harvested by freezing at −20°C for 3 h. Whole mosquitoes were individually homogenized (Retsch MM300 homogenizer, Retsch Inc., Newton, PA) in DMEM with 20% FBS and 250 μg/ml amphotericin B and stored at −80°C. Samples were centrifuged for 10 min at 5,000 rpm, and 75 μl of each sample supernatant were inoculated into 96-well plates containing Vero cells at 37°C and 5% $CO_2$ for 3 days, when they were fixed with a mixture of ice-cold acetone and methanol (1:1) solution and immunostained as described above. Infection was determined by detection of virus in the homogenized mosquito. The infection rate was recorded as the fraction of positive mosquitoes divided by the total number of engorged, incubated mosquitoes.

### Bio-Plex immuneassay.

Approximately $3\times10^5$ splenocytes were plated in 96-well plates and stimulated with $1.25\times10^4$ IFU ZIKV strain FSS13025 for 48 h. Culture supernatants were harvested and

cytokine production were measured using a Bio-Plex Pro Mouse Cytokine Assay (Bio-Rad, Hercules, CA).

### Intracellular cytokine staining (ICS).

Approximately $2.5\times10^6$ splenocytes were stimulated with $1\times10^5$ IFU live ZIKV (strain FSS13025) for 24 h. During the final 5 h of stimulation, BD GolgiPlug (BD Bioscience) was added to block protein transport. Cells were stained with antibodies for CD3, CD4, or CD8; fixed in 2% paraformaldehyde, and permeabilized with 0.5% saponin before addition of anti-IFN-γ, or control rat IgG1 (e-Biosciences). Samples were processed with a C6 Flow Cytometer instrument. Dead cells were excluded on the basis of forward and side light scatter. Data were analyzed with a CFlow Plus Flow Cytometer (BD Biosciences).

## Extended Data

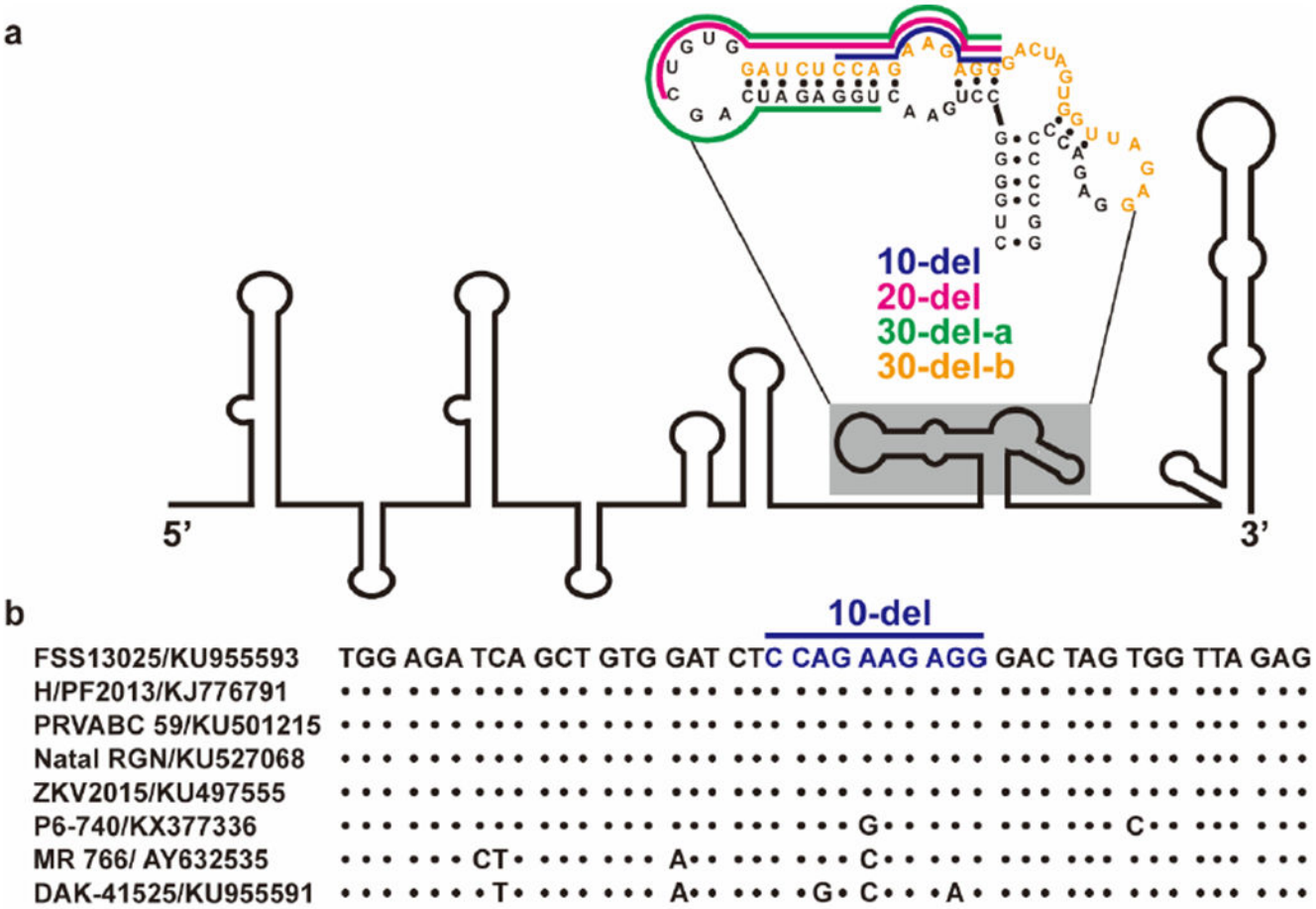


**Extended Data Figure 1. Predicted RNA structure of 3' UTR and sequence alignment of deleted nucleotides.**

**(a)** Predicted RNA secondary structure of ZIKV 3' UTR. The stem-loop structure of 3'UTR of ZIKV genome is presented as previously reported[33,34]. The nucleotide sequence of the shaded stem-loop is shown. The deleted sequences for 10-del, 20-del, 30-del-a, and 30-del-b mutants are displayed in blue, megaton, green, and orange, respectively. (b) Sequence

alignment of deleted region (nucleotide position 10,630-10,674) in 3'UTR. The 10-del nucleotides are indicated. Within the 10-del region, sequence variations are observed for early isolates (P6–740, MR766, and DAK-41525 were isolated in 1966, 1947, and 1984, respectively), while an identical sequence is observed for the strains isolated after 2010 (FSS13025, H/PF2013, PRVABC 59, Natal RGN, and ZKV2015).

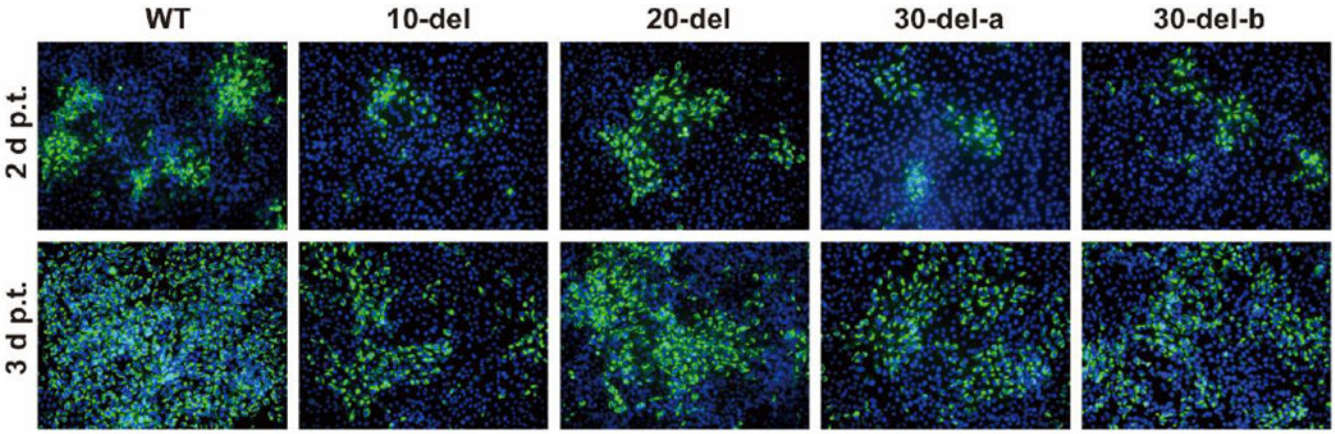


**Extended Data Figure 2. IFA of viral protein expression in cells transfected with WT or 3'UTR deletion ZIKV RNA.**

Vero cells were electroporated with 10 μg of genomic WT or 3'UTR deletion RNA of ZIKV. On day 2 and 3 post-transfection, IFA was performed to examine viral E protein expression using a mouse mAb (4G2) and Alexa Fluor® 488 goat anti-mouse IgG as the primary and secondary antibodies, respectively. Green and blue represent E protein and nuclei (stained with DAPI), respectively.

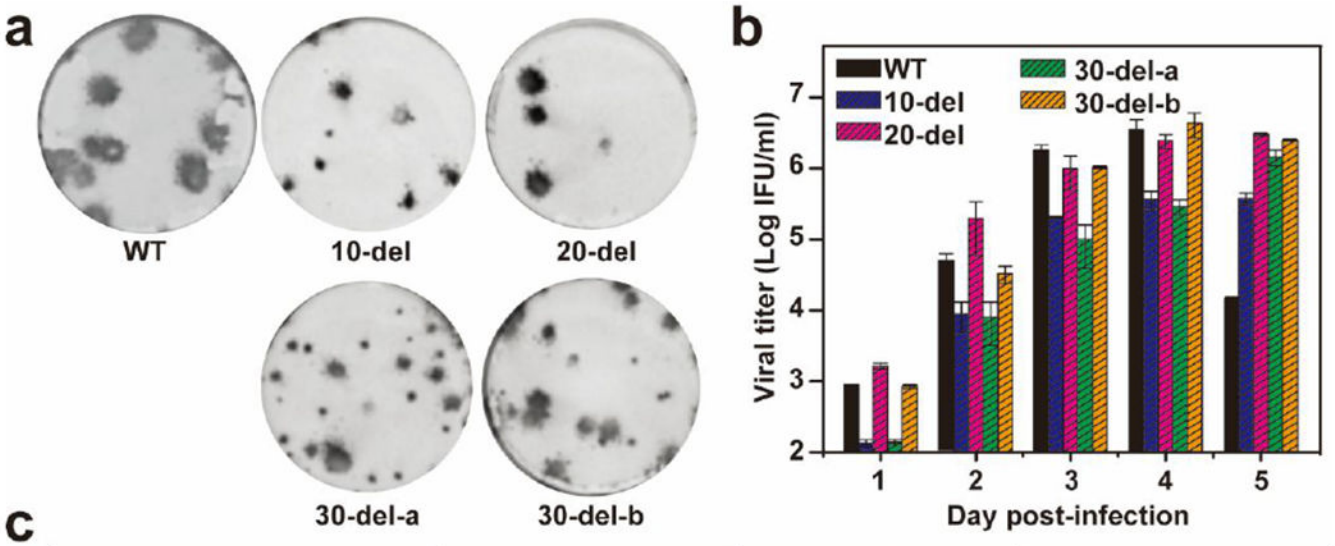


c

| | 10-del | | | 20-del | | | 30-del-a | | | 30-del-b | | |
|---|---|---|---|---|---|---|---|---|---|---|---|---|
| | I | II | III | I | II | III | I | II | III | I | II | III |
| E | R283W | H219L R283W L441L K443N | H219L | T315I | K443N | K443N | H401Y | H401Y | – | A501T | A501T | A501T |
| NS1 | | R103K | | | W98L | | | | | | | |

**Extended Data Figure 3. Stability analysis of the 3'UTR deletion ZIKVs in cell culture.**

P0 viruses (derived from the culture fluids of RNA-transfected cells from Fig. 1) were continuously cultured on Vero cells for five rounds (5 days for each round of culture), resulting in P5 viruses. The P5 viruses were subjected to the following characterization. (a) Immunostaining focus assay. WT and P5 mutant viruses were analyzed using an immunostaining focus assay on Vero cells. For each mutant virus, three independent selections were performed on Vero cells. Representative images of infectious foci for each P5 mutant virus are presented. (b) Replication kinetics. Vero cells in 24-well plates ($2\times10^5$ cells per well) were infected with WT and P5 mutant viruses at an MOI of 0.01. Culture fluids were quantified for infectious viruses on days 1 to 5 using the immunostaining focus assay on Vero cells. (c) Adaptive mutations in P5 mutant viruses. The complete genomes of P5 mutant viruses were sequenced for each of the three independent selections. The adaptive mutations are indicated by their amino acid positions of indicated genes based on ZIKV FSS13025 strain (GenBank number KU955593.1).

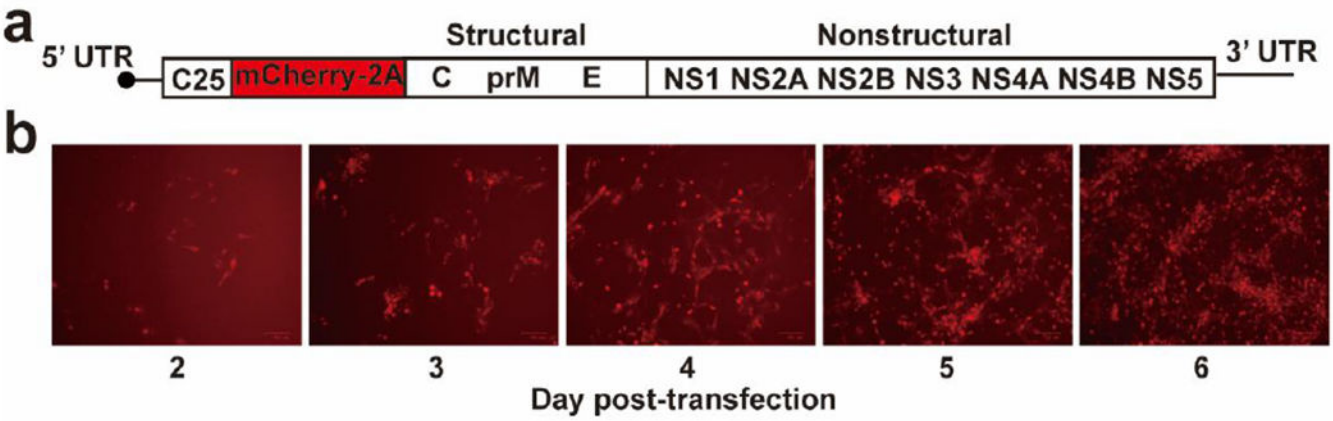


**Extended Data Figure 4. Construction of mCherry ZIKV.**

(a) Schematic genome of a mCherry ZIKV. A DNA fragment (encoding the first 25 amino acids of C gene, the mCherry gene, and the foot-and-mouth virus 2A protein) was in-frame fused with the open-reading-frame of ZIKV genome. (b) The mCherry expression in Vero cells transfected with mCherry ZIKV RNA. The expression of mCherry in transfected Vero cells was analyzed by a fluorescent microscopy at the indicated days post-transfection. The mCherry ZIKV was used to estimate antibody neutralization titers of mouse sera, as described in Methods.

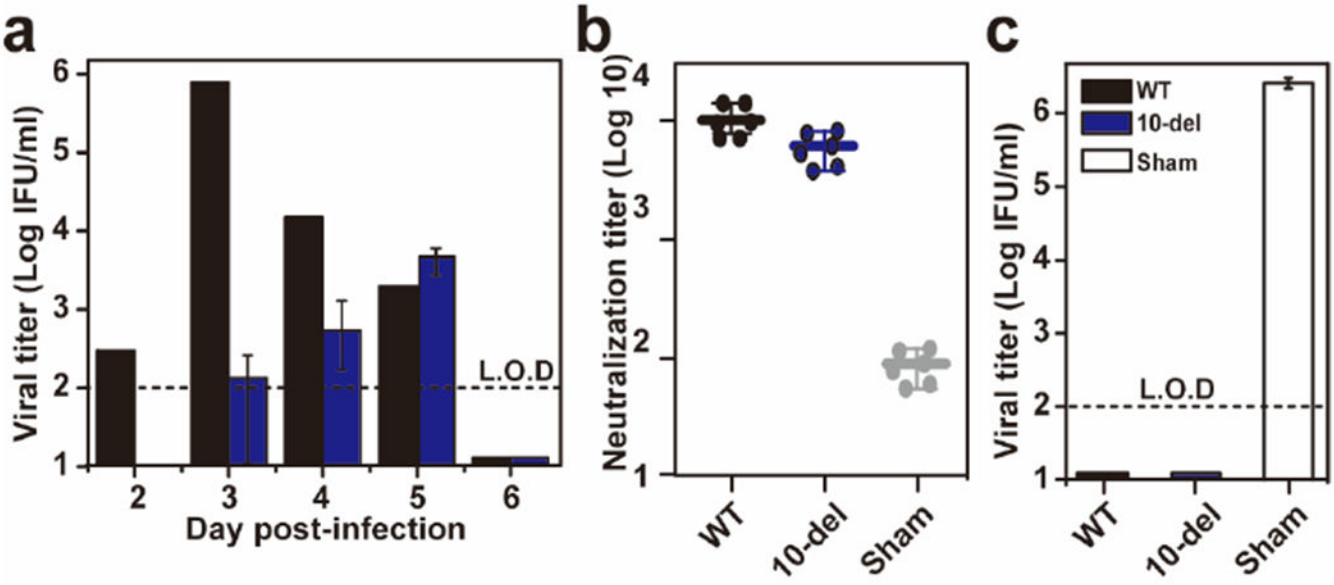


**Extended Data Figure 5. Efficacy of immunization with 100 IFU 10-del virus.**

(a) Viremia after immunization with 100 IFU of WT or 10-del ZIKV. Three-week-old A129 mice (n=5) were immunized with 100 IFU WT or 10-del virus via the S.C. route. Viremia were quantified by immunostaining focus assay from day 2 to 6. L.O.D., limit of detection. (b) Pre-challenge neutralization antibody titers. On day 28 post-immunization, mouse sera were quantified for ZIKV neutralizing antibody titers. (c) Viremia after challenge with ZIKV (Puerto Rico strain PRVABC59). On day 28 post-immunization, the mice were

challenged with $1\times10^6$ IFU of ZIKV via the I.P. route. Viremias were quantified by immunostaining focus assay on day 2 post-challenge.

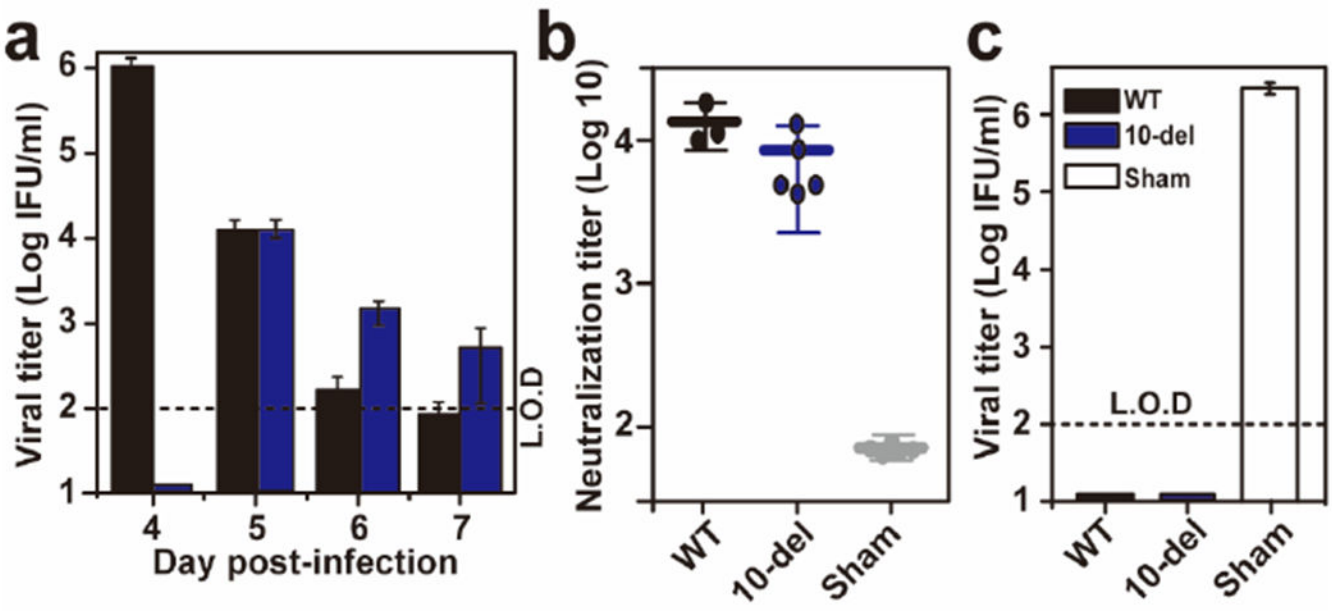


**Extended Data Figure 6. Efficacy of immunization with 10 IFU 10-del virus.**

(a) Viremia after immunization with 10 IFU of WT or 10-del ZIKV. Three-week-old A129 mice (n=5) were immunized with 10 IFU WT or 10-del virus via the S.C. route. Viremia were quantified by immunostaining focus assay from day 4 to 7. L.O.D., limit of detection. (b) Pre-challenge neutralization antibody titers. Three-week-old A129 mice (n=5) were immunized with 10 IFU 10-del ZIKV and PBS via the S.C. route. On day 28 post-immunization, mouse sera were quantified for ZIKV neutralizing antibody titers. (c) Viremia after challenge with epidemic ZIKV (Puerto Rico strain PRVABC59). On day 28 post-immunization, the mice were challenged with $1\times10^6$ IFU of ZIKV via the I.P. route. On day 2 post-challenge, viremias were quantified using an immunostaining focus assay.

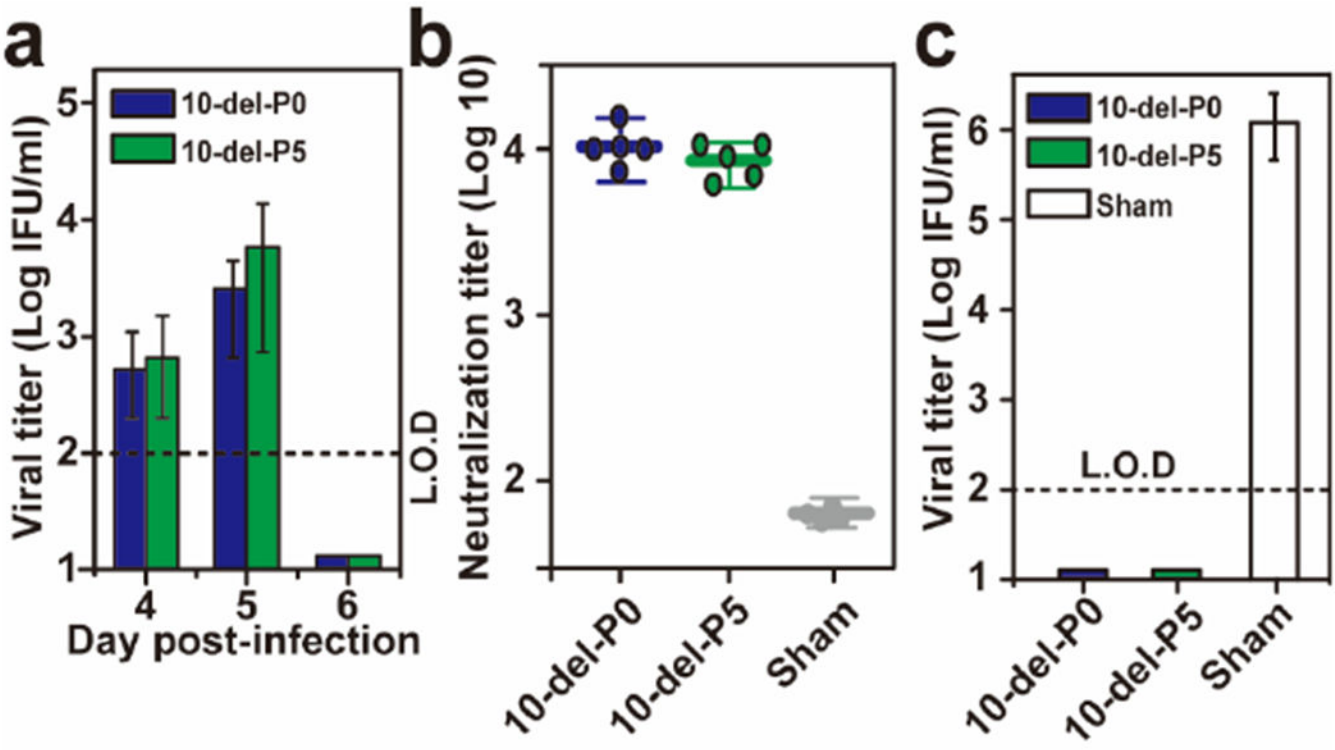


**Extended Data Figure 7. Comparison of viremia and efficacy of P0 and P5 10-del viruses.**

(a) Viremia after immunization with 100 IFU of P0 or P5 10-del ZIKV. Three-week-old A129 mice (n=5) were immunized with 100 IFU P0 or P5 10-del virus via the S.C. route. Viremia were quantified by immunostaining focus assay from day 4 to 6. L.O.D., limit of detection. (b) Pre-challenge neutralization antibody titers. On day 28 post-immunization, mouse sera were quantified for ZIKV neutralizing antibody titers. (c) Viremia after challenge with wild-type ZIKV. On day 28 post-immunization, the mice were challenged with $1\times10^6$ IFU of an epidemic strain of ZIKV (Puerto Rico strain PRVABC59) via the I.P. route. On day 2 post-challenge, viremias were quantified using an immunostaining focus assay.

## ACKNOWLEDGEMENTS

We thank our lab members and colleagues at University of Texas Medical Branch for helpful discussions during the course of this study. We are grateful to Mariano A. Garcia-Blanco and Shelton S. Brarick for providing lab space and equipment during the early stage of this work.

FUNDING SOURCES

P.Y.S. was supported by University of Texas Medical Branch (UTMB) startup award, UTMB Innovation and Commercialization award, University of Texas STARs Award, and a grant from Pan American Health Organization SCON2016–01353. This research was also supported by NIH grant AI120942 to S.C.W.

## REFERENCES

1. Costello A et al. Defining the syndrome associated with congenital Zika virus infection. Bull World Health Organ 94, 406–406A, doi:10.2471/BLT.16.176990 (2016). [PubMed: 27274588]

2. Weaver SC et al. Zika virus: History, emergence, biology, and prospects for control. Antiviral Res 130, 69–80, doi:10.1016/j.antiviral.2016.03.010 (2016). [PubMed: 26996139]

3. Shan C et al. Zika Virus: Diagnosis, Therapeutics, and Vaccine ACS Infectious Diseases 2, 170–172 (2016). [PubMed: 27623030]

4. Dawes BE et al. Research and development of Zika virus vaccines. npj Vaccines 1, 16007, doi: 10.1038/npjvaccines.2016.7 (2016). [PubMed: 29263851]

5. Barrett ADT Zika vaccine candidates progress through nonclinical development and enter clinical trials. Npj Vaccines 1, 16023, doi:10.1038/npjvaccines.2016.23 (2016). [PubMed: 29263861]

6. Larocca RA et al. Vaccine protection against Zika virus from Brazil. Nature 536, 474–478, doi: 10.1038/nature18952 (2016). [PubMed: 27355570]

7. Dowd KA et al. Rapid development of a DNA vaccine for Zika virus. Science 354, 237–240, doi: 10.1126/science.aai9137 (2016). [PubMed: 27708058]

8. Abbink P et al. Protective efficacy of multiple vaccine platforms against Zika virus challenge in rhesus monkeys. Science 353, 1129–1132, doi:10.1126/science.aah6157 (2016). [PubMed: 27492477]

9. Whitehead SS Development of TV003/TV005, a single dose, highly immunogenic live attenuated dengue vaccine; what makes this vaccine different from the Sanofi-Pasteur CYD vaccine? Expert review of vaccines 15, 509–517, doi:10.1586/14760584.2016.1115727 (2016). [PubMed: 26559731]

10. Shan C et al. An Infectious cDNA Clone of Zika Virus to Study Viral Virulence, Mosquito Transmission, and Antiviral Inhibitors. Cell Host Microbe 19, 891–900, doi:10.1016/j.chom. 2016.05.004 (2016). [PubMed: 27198478]

11. Xie X et al. Zika Virus Replicons for Drug Discovery. EBioMedicine 12, 156–160, doi:10.1016/ j.ebiom.2016.09.013 (2016). [PubMed: 27658737]

12. Lo L, Tilgner M, Bernard K & Shi P-Y Functional analysis of mosquito-borne flavivirus conserved sequence elements within 3' untranslated region of West Nile virus using a reporting replicon that differentiates between viral translation and RNA replication. J. Virol 77, 10004–10014 (2003). [PubMed: 12941911]

13. Pijlman GP et al.. A highly structured, nuclease-resistant, noncoding RNA produced by flaviviruses is required for pathogenicity. Cell Host Microbe 4, 579–591, doi:10.1016/j.chom. 2008.10.007 (2008). [PubMed: 19064258]

14. Manokaran G et al. Dengue subgenomic RNA binds TRIM25 to inhibit interferon expression for epidemiological fitness. Science 350, 217–221, doi:10.1126/science.aab3369 (2015). [PubMed: 26138103]

15. Acceptability of cell substrates for production of biologicals. Report of a WHO Study Group on Biologicals. World Health Organ Tech Rep Ser 747, 1–29 (1987). [PubMed: 3107222]

16. Rossi SL et al. Characterization of a Novel Murine Model to Study Zika Virus. Am J Trop Med Hyg 94, 1362–1369, doi:10.4269/ajtmh.16-0111 (2016). [PubMed: 27022155]

17. Govero J et al. Zika virus infection damages the testes in mice. Nature 540, 438–442, doi:10.1038/ nature20556 (2016). [PubMed: 27798603]

18. Ma W et al. Zika Virus Causes Testis Damage and Leads to Male Infertility in Mice. Cell 167, 1511–1524 e1510, doi:10.1016/j.cell.2016.11.016 (2016). [PubMed: 27884405]

19. Guerbois M et al. Outbreak of Zika Virus Infection, Chiapas State, Mexico, 2015, and First Confirmed Transmission by Aedes aegypti Mosquitoes in the Americas. J Infect Dis, doi:10.1093/ infdis/jiw302 (2016).

20. Ferreira-de-Brito A et al. First detection of natural infection of Aedes aegypti with Zika virus in Brazil and throughout South America. Mem Inst Oswaldo Cruz 111, 655–658, doi: 10.1590/0074-02760160332 (2016). [PubMed: 27706382]

21. Yun SI et al. Comparison of the live-attenuated Japanese Encephalitis vaccine SA14–14-2 strain with Its pre-attenuated virulent parent SA14 strain: Similarities and differences in vitro and in vivo. J Gen Virol, doi:10.1099/jgv.0.000574 (2016).

22. Barrett AD & Gould EA Comparison of neurovirulence of different strains of yellow fever virus in mice. J Gen Virol 67 (Pt 4), 631–637, doi:10.1099/0022-1317-67-4-631 (1986). [PubMed: 3958694]

23. Khromykh AA, Sedlak PL & Westaway EG Trans-Complementation analysis of the flavivirus Kunjin ns5 gene reveals an essential role for translation of its N-terminal half in RNA replication. J. Virol 73, 9247–9255 (1999). [PubMed: 10516033]
24. Khromykh A, Kenney M & Westaway E trans-Complementation of flavivirus RNA polymerase gene NS5 by using Kunjin virus replicon-expressing BHK cells. J. Virol 72, 7270–7279 (1998). [PubMed: 9696822]
25. Qing M, Liu W, Yuan Z, Gu F & Shi PY A high-throughput assay using dengue-1 virus-like particles for drug discovery. Antiviral Res 86, 163–171 (2010). [PubMed: 20153777]
26. Xie X, Zou J, Puttikhunt C, Yuan Z & Shi PY Two distinct sets of NS2A molecules are responsible for dengue virus RNA synthesis and virion assembly. J Virol 89, 1298–1313, doi:10.1128/JVI.02882-14 (2015). [PubMed: 25392211]
27. Pugachev K et al. High fidelity of yellow fever virus RNA polymerase. J. Virol 78, 1032–1038 (2004). [PubMed: 14694136]
28. Xie X et al. Understanding Zika Virus Stability and Developing a Chimeric Vaccine through Functional Analysis. mBio In press (2017).
29. Yauch LE et al. A protective role for dengue virus-specific CD8+ T cells. J Immunol 182, 4865–4873, doi:10.4049/jimmunol.0801974 (2009). [PubMed: 19342665]
30. Weiskopf D et al. Comprehensive analysis of dengue virus-specific responses supports an HLA-linked protective role for CD8+ T cells. Proc Natl Acad Sci U S A 110, E2046–2053, doi:10.1073/pnas.1305227110 (2013). [PubMed: 23580623]
31. Shi PY, Tilgner M, Lo MK, Kent KA & Bernard KA Infectious cDNA clone of the epidemic West Nile virus from New York City. J. Virol 76, 5847–5856 (2002). [PubMed: 12021317]
32. Hansen DA, Esakky P, Drury A, Lamb L & Moley KH The aryl hydrocarbon receptor is important for proper seminiferous tubule architecture and sperm development in mice. Biol Reprod 90, 8, doi:10.1095/biolreprod.113.108845 (2014). [PubMed: 24174576]
33. Ye Q et al. Genomic characterization and phylogenetic analysis of Zika virus circulating in the Americas. Infect Genet Evol 43, 43–49, doi:10.1016/j.meegid.2016.05.004 (2016). [PubMed: 27156653]
34. Akiyama BM et al. Zika virus produces noncoding RNAs using a multi-pseudoknot structure that confounds a cellular exonuclease. Science 354, 1148–1152, doi:10.1126/science.aah3963 (2016). [PubMed: 27934765]

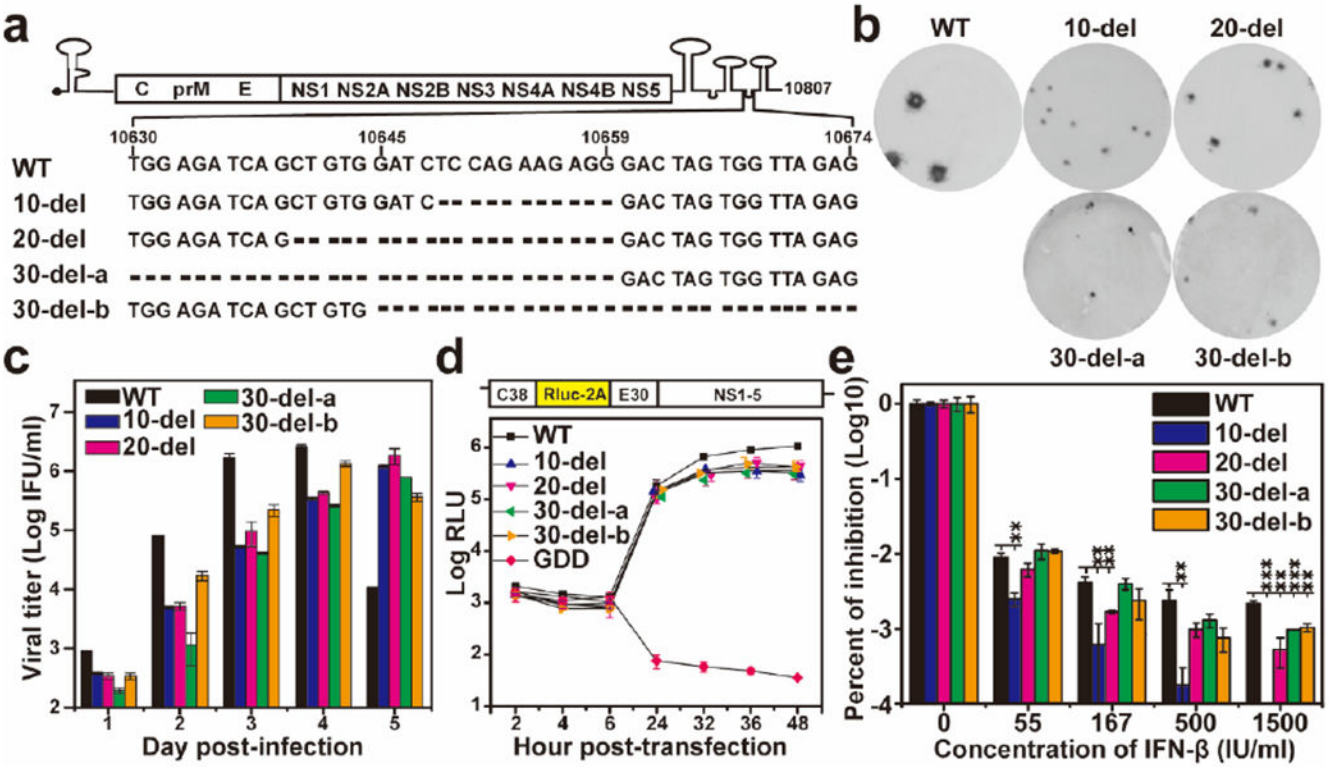


**Figure 1. Characterization of the 3'UTR deletion mutants in cell culture.**

(a) Sequences of the ZIKV 3'UTR deletions. (b) Immunostaining focus assay of mutant viruses. Equal amounts of RNAs (10 μg) transcribed from their corresponding infectious cDNA clones were electroporated into Vero cells. On day 4 or 5 post-transfection, culture fluids form the transfected cells were harvested and quantified for infectious viruses (defined as P0 virus ) using an immunostaining focus assay on Vero cells. (c) Replication kinetics of WT and mutant viruses. Vero cells in 24-well plates ($2\times10^5$ cells per well) were infected with WT and mutant viruses at an MOI of 0.01. Culture fluids were quantified for infectious viruses on days 1 to 5 using the immunostaining focus assay. (d) Replicon analysis of the 3'UTR deletions. A *Renilla* luciferase reporter replicon of ZIKV (top panel) was engineered with various 3'UTR deletions. Equal amounts of replicon WT and mutant RNAs (10 μg) were electroporated into Vero cells. Luciferase signals were measured at the indicated time points (bottom panel). A non-replicative replicon containing an NS5 polymerase-inactive GDD mutation was included as a negative control. The averages of three replicates are presented. Error bars represent standard deviations. RLU, relative light units. (e) Interferon-β inhibition of WT and mutant ZIKVs. Vero cells were seeded in 96-well plate ($1.5\times10^4$ cell per well) one day before interferon treatment and viral infection. The cells were infected at an MOI 0.05 in the presence of IFN-β (55, 167, 500, or 1,500 IU/ml). Viral infection and interferon treatment were initiated at the same time. At 48 h post-infection and interferon-β treatment, viral titers were quantified using the immunostaining focus assay on Vero cells. Percentages of viral titer inhibition are presented in $\log_{10}$ scale. Viral titers without interferon-β treatment are set as 100%. Average results of three independent experiments are shown. Error bars represent standard deviations. Symbols ** and *** indicate *P* values <0.01 and <0.001, respectively.

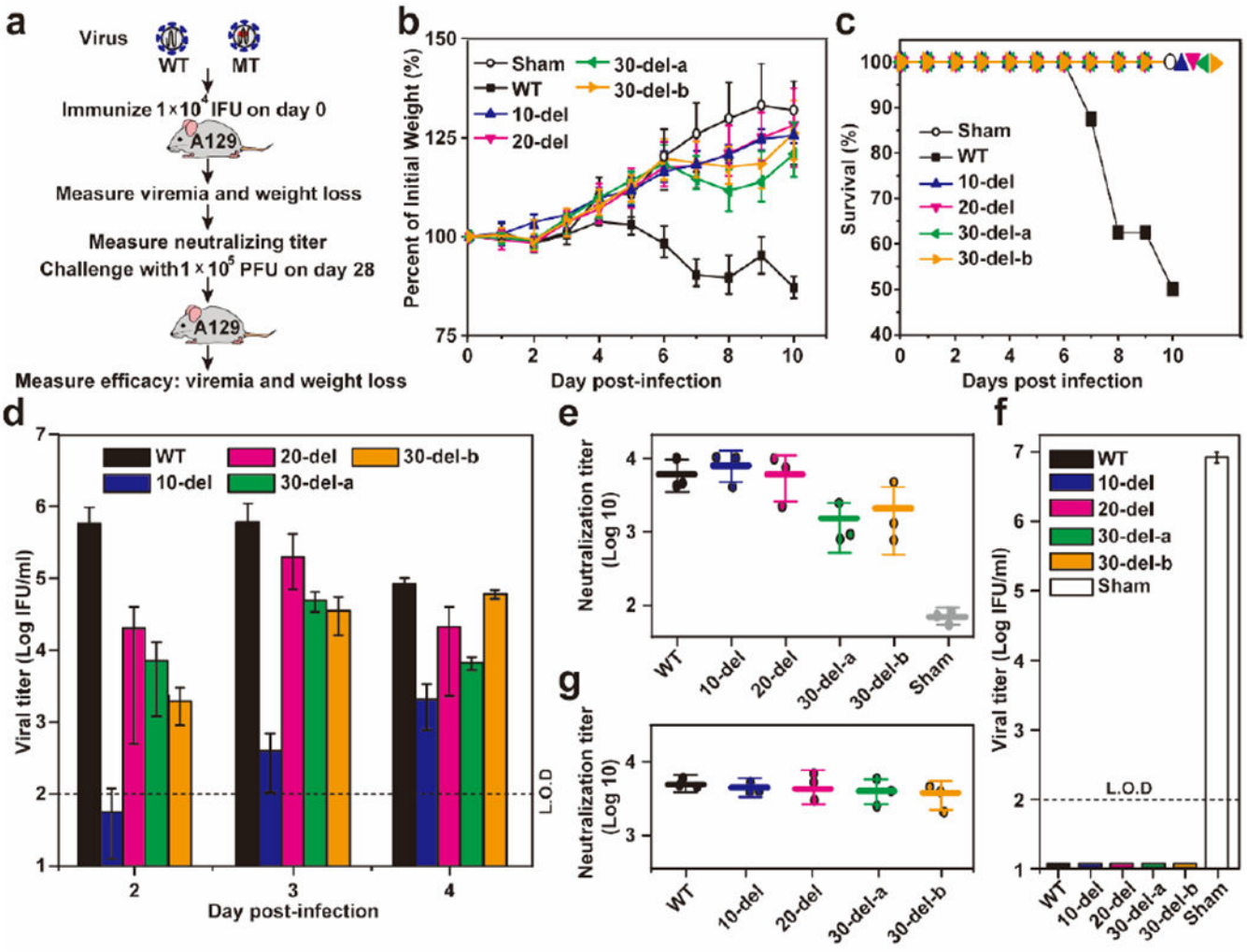


**Figure 2. Characterization of 3'UTR mutants in the A129 mouse model.**

(a) Experimental scheme. In two separate experiments, three-week old A129 mice (n=8) were immunized via the S.C. route with $1\times10^4$ IFU WT and mutant viruses. The immunized mice were monitored for weight loss (b), survival (c), and viremia (d). Weight loss is indicated by percentage using the weight on the day before immunization as 100%. Viremias were quantified by an immunostaining focus assay from day 2 to 4 post-infection. (e) Pre-challenge neutralization antibody titers. On day 28 post-immunization, mouse sera were measured for neutralizing titers using a mCherry ZIKV infection assay (Extended data Fig. 4). (f) Post-challenge viremia. On day 28 post-immunization, mice were challenged with $1\times10^5$ PFU parental virus (ZIKV strain FSS13025) via the I.P. route. Viremia on day 2 post-challenge was quantified using the immunostaining focus assay. (g) Post-challenge neutralization antibody titer. On day 28 post-challenge, mouse sera were quantified for neutralizing titers using the mCherry ZIKV infection assay. L.O.D.: limit of detection.

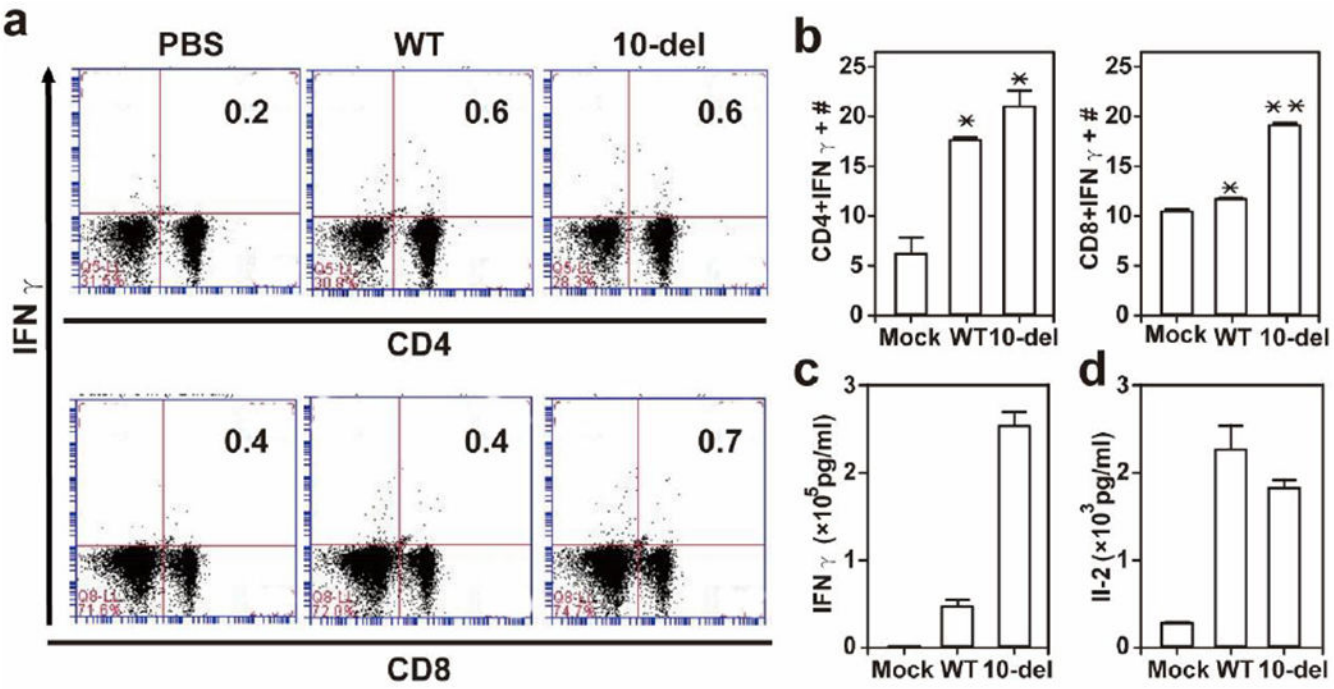


**Figure 3. T cell responses after primary infection with ZIKV WT or 10-del mutant.**

A129 mice were infected with $1\times10^4$ IFU WT and 10-del viruses. On day 28 post-infection, mouse spleens were harvested. Splenocytes were counted, cultured *ex vivo* with WT ZIKV for 24 h, and stained for markers (IFN-γ, CD3, and CD4 or CD8). The T cells were gated, and percentages of $CD4^+IFN\text{-}\gamma^+$ cells and $CD8^+IFN\text{-}\gamma^+$ are shown (a). Total number of T cell subsets per spleen is shown (b). Supernatants from the *ex vivo* culture were harvested on day 2 after WT ZIKV restimulation, and measured for IFN-γ (c) and IL-2 (d) production. Data are presented as means ± SEM, n = 2–4 per group. $*P < 0.05$ or $**P < 0.01$ difference between the virus- and mock-infected mice.

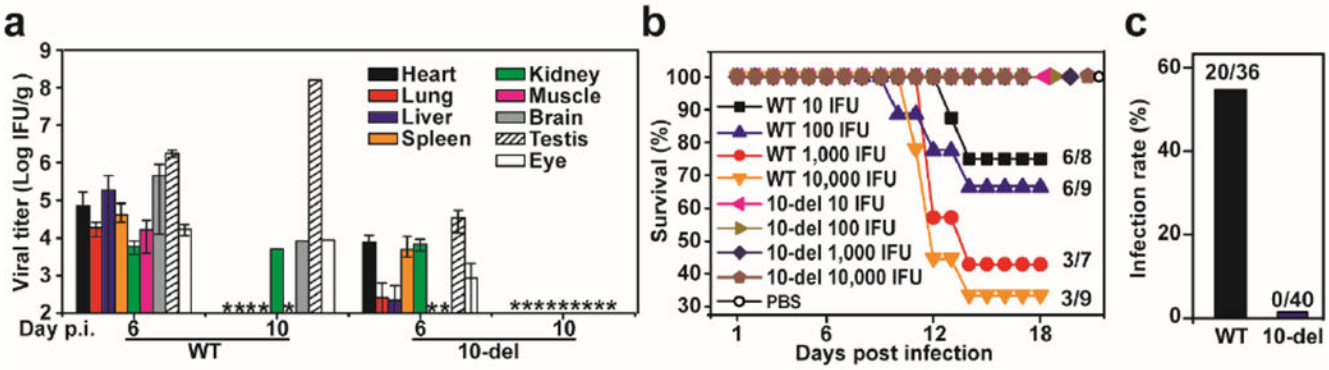


**Figure 4. Safety evaluation of 10-del virus.**

(a) Viral loads in organs of infected A129 mice. Three-week-old A129 mice were immunized with $1\times10^4$ IFU of WT and 10-del viruses. Organs from infected mice were collected and homogenized on day 6 and 10 post-infection. The amounts of viruses were quantified on Vero cells using an immunostaining focus assay. The mean results from three animals are presented. Bars denote standard errors. "?*" denotes no detectable virus. (b) Sperm count analysis of A129 mice infected with WT or 10-del mutant virus. Male A129 mice were infected with $1\times10^4$ IFU of WT and 10-del viruses (n=4 per group). On day 16 p.i., epididymis was harvested for sperm count analysis. Total sperm counts and motile sperm counts were measured. One-way ANOVA test was performed to indicate statistical significance among different infection groups. n.s., not significant; ***very significant ($p$ value <0.001); ****extremely significant ($p$ value <0.0001). In addition, testes were harvested and weighted. No statistic difference in testis weight was detected from the WT-, 10-del-, and mock-infected mice (data not shown). (c) Comparison of neurovirulence of WT and 10-del viruses in CD1 newborn mouse. Groups of one-day-old CD1 mice (n=7–10) were injected via the I.C. route with 10 to $1\times10^4$ IFU of WT or 10-del virus. (d) Mosquito infectivity assay. *Aedes aegypti* were fed with WT or 10-del virus on artificial blood-meals. On day 7 post-feeding, individual engorged, incubated mosquitoes were homogenized and infection was assayed by immunostaining of viral protein expression on inoculated Vero cells (see Methods for details). The number of infected mosquitos and total number of engorged mosquitoes are indicated.